Product state analysis of BaO from the reactions Ba + CO_2 and Ba + O_2

P. J. Dagdigian*, H. W. Cruse†, A. Schultz‡, and R. N. Zare

Department of Chemistry, Columbia University, New York, New York 10027
(Received 19 July 1974)

The reactions Ba + O_2 → BaO + O and Ba + CO_2 → BaO + CO have been investigated using the method of laser-induced fluorescence to detect the BaO products. Excitation spectra of BaO produced under single-collision conditions in these reactions are reported, and initial rotational population distributions for BaO formed in the $v=0$ vibrational level are deduced. The BaO excitation spectrum from the reaction Ba + CO_2 shows clear band heads and rotationally resolved features which can all be assigned. By contrast, the Ba + O_2 excitation spectrum is markedly more complex since the band heads are missing and many high (v, J) levels are populated. The BaO rotational distributions for both reactions are found to be nonthermal, based on comparisons with simulated spectra. Estimates of the initial vibrational populations are also obtained. By extrapolation of the highest observed ($v = 0$, J) levels populated in the Ba + CO_2 reaction, the dissociation energy of BaO has been determined to be D_0^0 (BaO) = 133.5 ± 1.3 kcal/mole. Since molecular beam investigations have shown that the Ba + O_2 reaction proceeds through a long-lived collision complex, the experimental $v = 0$ rotational distributions have been compared with those calculated by phase space theory and transition state theory. The previous treatments of these statistical models have been extended to four-atom complexes. The results of the transition state theory reproduce the qualitative features of the experimental distributions, while the results of the phase space theory are in remarkable agreement with experiment. This strongly suggests that the dynamics of both reactions are governed by the formation of a long-lived collision complex.

I. INTRODUCTION

We report here the internal state distributions of the BaO products formed by the Ba + O_2 and Ba + CO_2 reactions under single-collision conditions. These distributions are determined from laser-induced fluorescence excitation spectra. A preliminary report[1] on the Ba + O_2 reaction has already appeared. The present paper refines and also corrects the BaO distribution obtained from these earlier experiments since we have found that the previous experiments suffered significantly from collisional relaxation of the internal states of the reaction products between the time of formation and detection.

A number of molecular beam scattering experiments have also been reported on the Ba + O_2 reaction.[2–4] While there is some disagreement on the angular distribution of the BaO product, the most recent experiment by Loesch and Herschbach[4] indicates that at initial relative kinetic energies of 2–17 kcal/mole the center-of-mass angular distribution shows approximately symmetrical forward–backward peaking. This implies that the collision complex is long-lived compared to its rotational period. The internal state distributions provide complementary information on Ba + O_2 and also yield information on Ba + CO_2, for which no angular distribution measurements have been reported.

It appears that the best-studied example of a long-lived collision complex is the reaction Cs + SF_6. Not surprisingly for this 8-atom complex, the translational,[5] vibrational,[6] and rotational[7] distributions are found to be well characterized by temperatures, indeed by nearly the same temperature. The reaction systems under study here are perhaps presently the best examples of long-lived complexes that have few degrees of freedom. By contrast, their internal state distributions show marked departures from a Boltzmann distribution. Consequently these distributions serve as a sensitive test of various statistical theories. We present here a comparison with the predictions of phase space theory and transition state theory, where we assume the entrance and exit channels are dominated by centrifugal barriers rather than activation barriers. We find that both theories predict distributions qualitatively similar to the experimental distribution but that the phase space theory agrees quite closely.

II. APPARATUS

A number of improvements have been made to the apparatus since the preliminary BaO spectra were reported.[1] First, differential pumping between the oven and scattering chambers has been increased. This improvement was necessary so that reasonable reagent gas pressures ($\leq 1\times10^{-4}$ torr) could be used without causing appreciable collisional relaxation of the initial BaO internal state distribution by forming BaO molecules in the oven chamber and by allowing a number of secondary collisions associated with a longer effective path length. A new scattering chamber, an aluminum box $86\times40\times40$ cm in dimension, has been constructed for this purpose. This chamber is evacuated by a Varian NRC VHS-6 oil diffusion pump (pumping speed 1600 liters/sec with baffle). The old reaction chamber, now used as the oven vacuum chamber, is attached to the end of the scattering chamber. The two chambers are isolated from each other by a bulkhead flange, which has a slit, 0.2×2 cm in size, through which the Ba beam passes.

A new Ba beam source has also been constructed. Light from the heater wires in the previous source was a large dc contribution to the photomultiplier signal and put a restrictive limit on the high voltage applied to the tube and hence limited the gain. The present source, similar in design to the alkali dimer source of

Dagdigian and Wharton,[8] consists of a molybdenum crucible, 1.9 cm in diameter and 8 cm long, which is placed inside a molybdenum heater tube, 2.5 cm in diameter and 17 cm long. Because of the large radiative area of the heater tube, its temperature is not appreciably higher than that of the crucible, unlike that of heater wires. The Ba charge is maintained at a temperature of 1050 °K, corresponding to a Ba vapor pressure of 0.3 torr,[9] while the source orifice (0.3 cm in diameter) is at 1200 °K (corrected pyrometer readings). The bulkhead flange separating the chambers is located 2.5 cm from the Ba source, and the laser excitation zone is located 6 cm from the flange.

BaO is produced by adding O_2 at pressures of $\leq 1 \times 10^{-4}$ torr in the scattering chamber while allowing the Ba beam to enter ("beam + gas" arrangement). The presence of O_2 is essentially uniform throughout the scattering chamber so that ionization gauge readings appropriately indicate the pressure in the reaction zone. In the present setup there is a small amount of leakage into the oven chamber; with a pressure of O_2 of 1×10^{-4} torr in the reaction chamber, the pressure rise in the oven chamber is 2×10^{-6} torr (uncorrected ionization gauge readings). Nevertheless the BaO fluorescence signal disappears as soon as the O_2 gas is turned off. Thus, this indicates that a negligible fraction of BaO molecules originates from "oven reaction"[10] in the oven vacuum chamber.

The fluorescence excitation and detection equipment are very similar to that used in previous experiments.[11] The earlier runs employed the pulsed dye laser system previously described, in which an Avco C950 nitrogen laser (100 kW peak power) pumps an Avco dye module (10 pps). It was necessary to shield the nitrogen laser because of rf interference. The dye module was modified, as described previously. With an Oriel 20X intracavity beam expanding telescope, we achieved bandwidths of 0.5 Å. Wavelength scans of the laser were performed using a variable-speed clock motor. In later runs the nitrogen laser and dye module employed were the Molectron UV-300 nitrogen laser (300 kW peak power) and the DL-200 dye module (20 pps). Once again, it was necessary to shield extensively the nitrogen laser in order to minimize rf pickup. Also the same motor drive was employed.

The dyes used (solutions in ethanol) with the Avco system were brilliant sulphaflavine (5150–5500 Å), rhodamine 6G (5700–5900 Å), rhodamine B (5975–6150 Å), and 7-diethylamino-4-methylcoumarin (4500–4800 Å). With the Molectron system, the dyes used were fluoral 7GA[12] (GAF Corporation), which was recrystallized in ethanol (5300–5600 Å), and CSA-22[13] (5100–5400 Å). It was necessary to add 7-diethylamino-4-methylcoumarin to both dyes to maximize laser power; the bandwidths with both dyes were about 0.3 Å.

Full laser power is employed because of the low intensity of the BaO fluorescence signals. Consequently, no studies of the effect of optical pumping have been made, as done in previous experiments. Optical pumping is expected to affect the relative intensities of vibrational bands if the Franck–Condon factors are markedly different but not to alter appreciably rotational line intensities in a given band.

It is possible with the present reaction chamber to move the photomultiplier (RCA 7265, S-20 photocathode) much closer to the laser excitation zone than in previous experiments.[11] With the photomultiplier 5 cm from the excitation zone, about 5% of the fluorescence strikes the photocathode and hence the collection efficiency is a factor of 10 greater than before. A PAR model 160 boxcar integrator is used to amplify and average the fluorescence signals. Since the radiative lifetime of the A state of BaO is about 350 nsec,[1,14] a gate width of 1 μsec is used. The gate is opened just before the beginning of the laser pulse since it is found that scattered laser light is not an appreciable fraction of the observed signal. The fluorescence is not spectrally resolved.

III. RESULTS

The BaO reaction product is detected using laser-induced fluorescence of the $A\ ^1\Sigma^+ - X\ ^1\Sigma^+$ band system. Figures 1 through 4 show typical scans of BaO fluorescence as a function of laser wavelength (excitation spectra) for the reactions $Ba + O_2$ and $Ba + CO_2$. Because of the complexity of these spectra, we choose to concentrate our attention on the form of the rotational distribution of the $v'' = 0$ vibrational level. Consequently, the most convenient bands proved to be the (4, 0) and (5, 0) because they have the least interference from overlapping $v'' \neq 0$ bands and from the intense Ba resonance line at 5535 Å. First we review briefly the derivation of relative rotational populations from excitation spectra. Then we apply these formulas to the $Ba + CO_2$ reaction and then to the $Ba + O_2$ reaction since the spectrum of the former is much less complicated.

The fluorescent line intensity $I(v'J';v''J'')$ (energy/sec) corresponding to excitation from the lower (v'', J'') vibration–rotation level to the upper (v', J') level is given in the Born–Oppenheimer approximation by

$$I(v'J'; v''J'') = k\{N_{v''J''}\rho[\lambda(v'J'; v''J'')]q_{v'v''} \times S_{J'J''}/(2J''+1)\}\sum_{v} \nu_{v'v}^4 q_{v'v} P(\lambda_{v'v}) , \quad (1)$$

where $N_{v''J''}$ is the population of the (v'', J'') level (summed over M_J magnetic sublevels), $\rho[\lambda(v'J'; v''J'')]$ is the laser energy density (energy/cm^3) at the wavelength $\lambda(v'J'; v''J'')$ of the $v''J'' \rightarrow v'J'$ transition, q and ν are the Franck–Condon factor[15] and frequency, respectively, for the vibrational band denoted by the subscripts, $S_{J'J''}$ is the line strength[16] for the $J'' \rightarrow J'$ transition, $P(\lambda_{v'v})$ is the (energy) sensitivity of the photomultiplier at the wavelength $\lambda_{v'v}$ of the (v', v) band, and k is a proportionality constant which includes geometric factors and the assumed constant[17] electronic transition moment. In Eq. (1), the term in braces represents the absorption process, while the summation accounts for the emission branches, For a $^1\Sigma^+ - {}^1\Sigma^+$ band system, the only nonzero values for $S_{J'J''}$ are $J''+1$ if $J' = J''+1$ (R branch) and J'' if $J' = J''-1$ (P branch). While it is known[18] that the upper $A\ ^1\Sigma^+$ state of BaO is

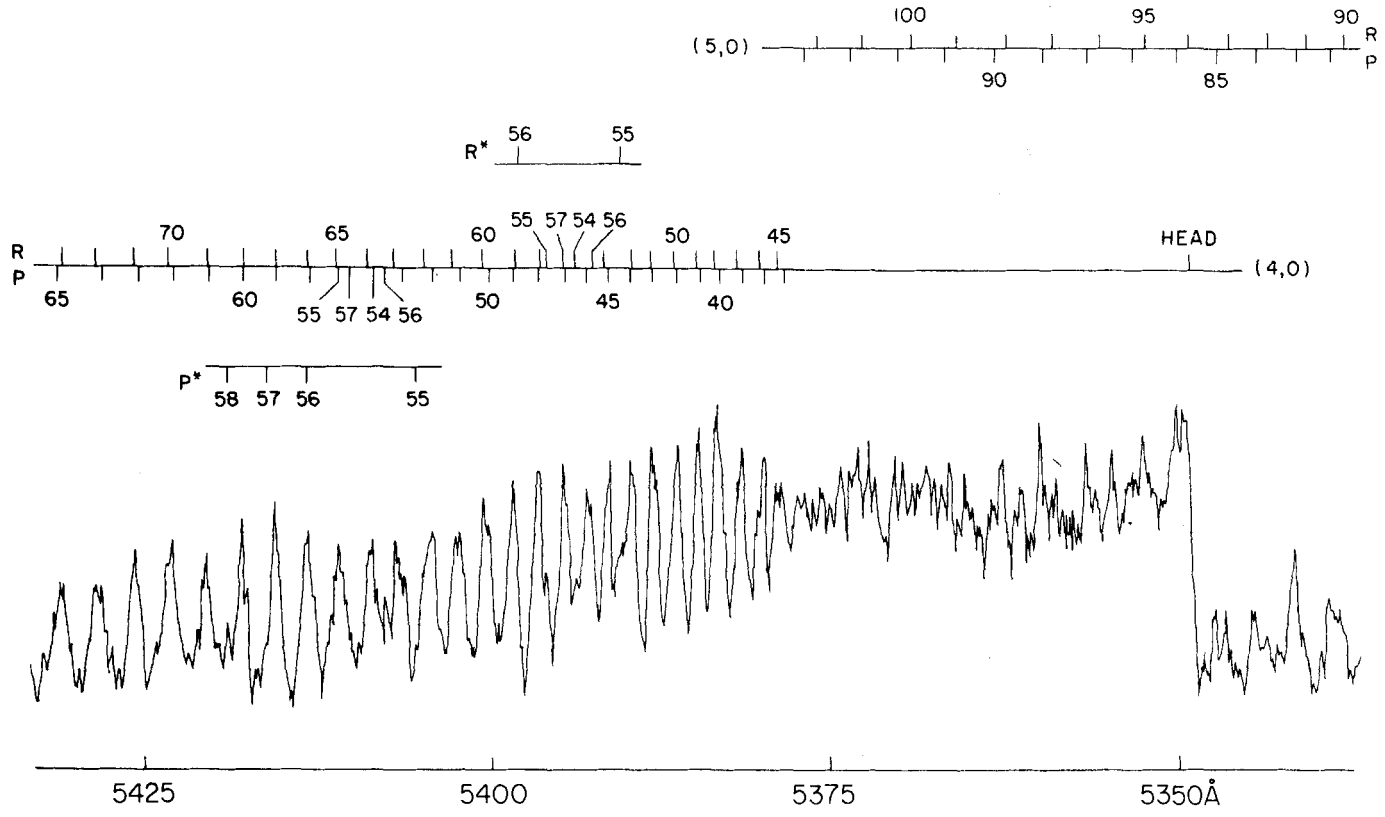

FIG. 1. BaO excitation spectrum for the reaction Ba + CO_2 → BaO + CO. The rotational lines of the $A\,^1\Sigma^+ - X\,^1\Sigma^+$ (4, 0) and (5, 0) bands are marked; $R(J'')$ and $P(J'')$ identifies lines for which $J' = J'' + 1$, and $J' = J'' - 1$, respectively. The presence of electronic perturbations in the A state is obvious from the displacement of some lines and the appearance of new lines. The spectrum was taken with the Avco dye module (brilliant sulphaflavine dye, bandwidth 0.5 Å).

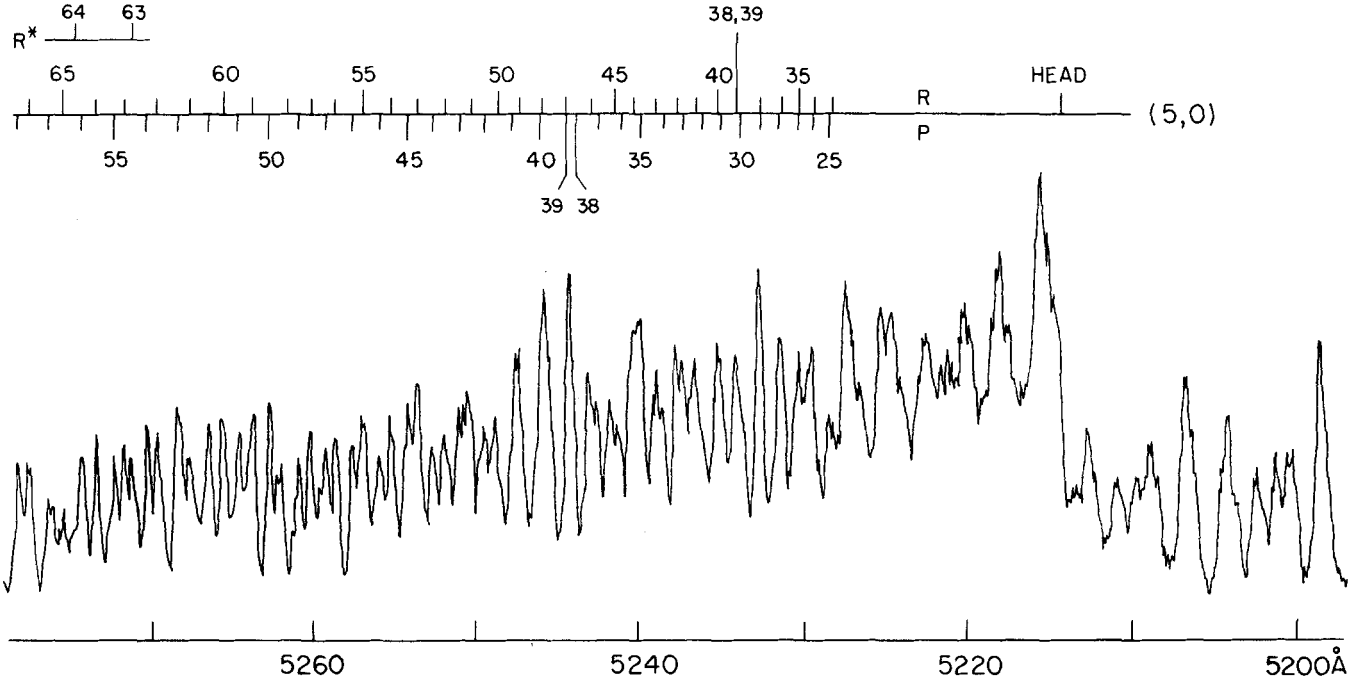

FIG. 2. BaO excitation spectrum for the Ba + CO_2 reaction. The spectral region around the (5, 0) band head is shown. Lines from bands other than (5, 0) have not been marked since their identification is uncertain. The spectrum was taken with the Molectron dye module (CSA-22 dye, bandwidth 0.3 Å).

electronically perturbed, Eq. (1) is sufficiently accurate for rotational lines far from the perturbations. It is possible, in principle, to obtain the rotational distribution in a given v'' level from the line intensities of either the R or the P series. We note from Eq. (1) that to a good approximation,

$$I(v''J_1''; v'J_1'' \pm 1)/I(v''J_2''; v'J_2'' \pm 1) = N_{v''J_1''}/N_{v''J_2''} \qquad (2)$$

for large J, that is, the ratio of intensities of either P or R lines, respectively, in some band gives directly the ratio of the populations of rotational states in the same v'' level. Moreover, Eq. (2) permits a simple experimental check in that the populations obtained from corresponding P and R series should agree.

A. The Ba + CO_2 reaction

As can be seen in Figs. 1 and 2, the BaO excitation spectrum from this reaction is fairly simple. It is possible to assign virtually all observed rotational lines using the published spectroscopic data of Lagerqvist, Lind, and Barrow.[18] Only low v'' levels and moderate J'' states are significantly populated. Band heads ($J_{head} \sim 5$) are clearly discernible although they are not sharp.

Because of the ralatively wide laser bandwidth (0.3–0.5 Å), a large fraction of the rotational lines of a band, particularly those near the band head, are not individually resolved. However, the rotational distribution may be deduced by comparing the experimental spectrum with simulated spectra obtained by convoluting the rotational lines with the laser bandwidth function. A computer program has been written for this purpose. Rather than inserting all the measured line positions in the convolution program, we have taken account of the rotational perturbations by using Field's analysis.[19] Fortunately in the $v' = 4$ and 5 levels of the A state the perturbations are isolated so that the line positions may be calculated by diagonalizing a 2×2 Hamiltonian which expresses the interaction between the A state rotational level and the particular perturbing level. In this manner, we also obtain the fraction of A state character for these J' levels. Since the perturbing states have negligible transition moments to the X state compared to the A–X transition moment, the perturbations have the effect of reducing the transition moment. Hence, the expression for the intensity $I(v'J'; v''J'')$ given in Eq. (1) must be multiplied by the fraction of A state character for a perturbed J' level. The rotational constants determined by molecular beam microwave resonance spectroscopy[20] for the X state and those determined by microwave optical double resonance[21] for the A state are used here. As an indication of the adequacy of Field's analysis we note that the experimental line positions are reproduced to an average deviation of 1.2 and 0.3 cm^{-1} in the (4, 0) and (5, 0) bands, respectively, and the maximum deviations are ± 2 cm^{-1}. For many lines in the (4.0) bands, it is necessary to adjust the calculated term values based on Field's analysis so that the deviation is small compared to the laser bandwidth. The laser bandwidth function is sufficiently approximated by a Gaussian with the experimental FWHM.

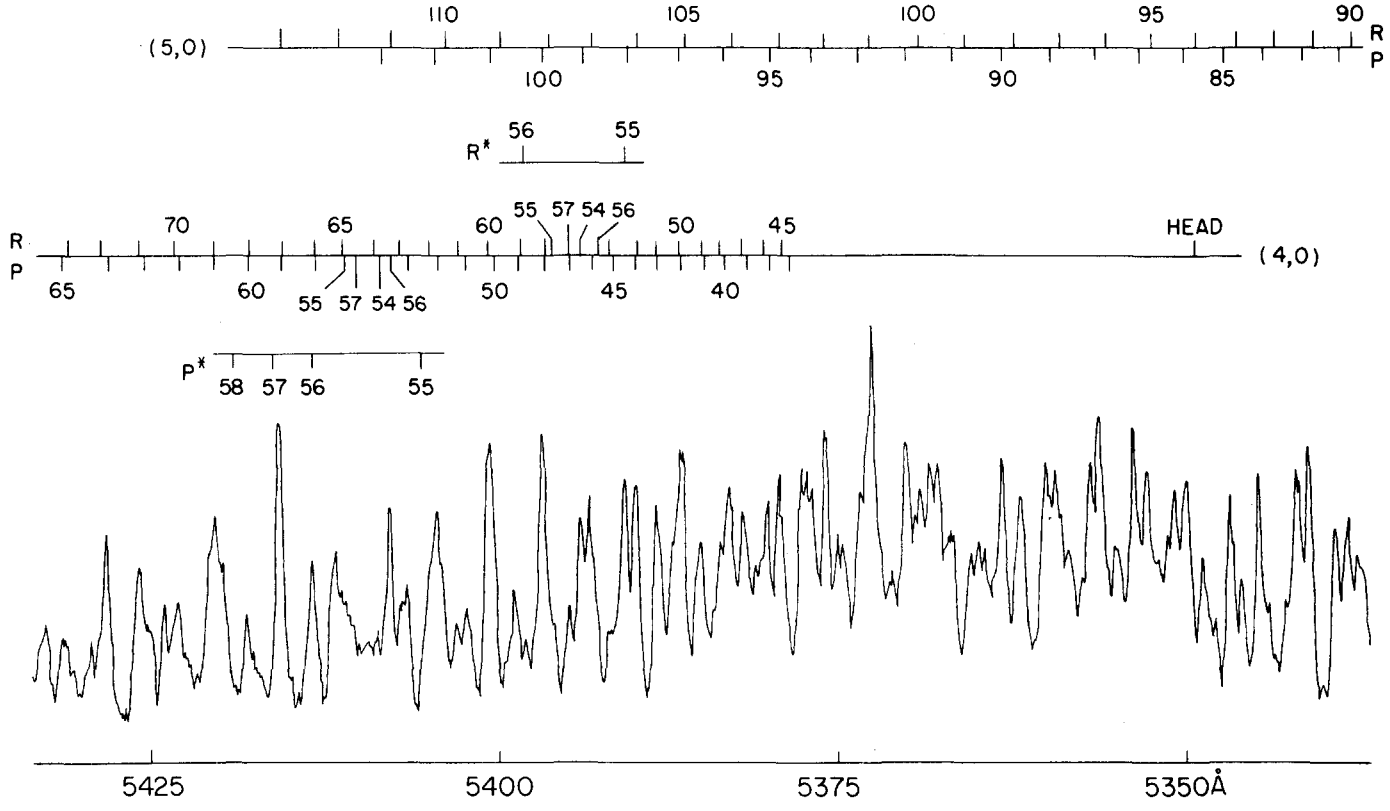

FIG. 3. BaO excitation spectrum for the reaction Ba + O_2 → BaO + O. The spectral region shown is the same as in Fig. 1, and the same operating conditions were used.

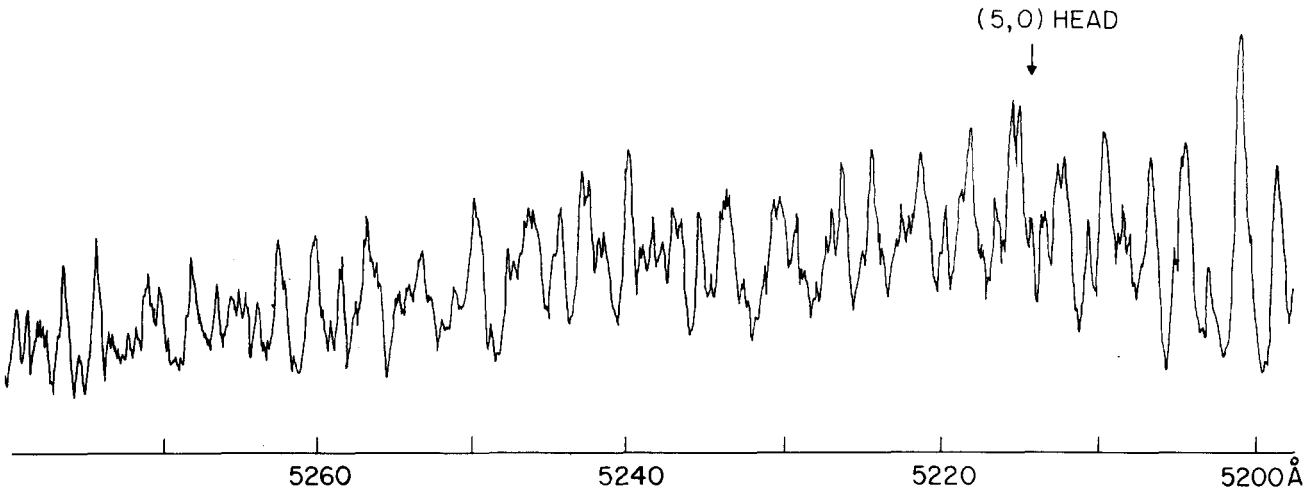

FIG. 4. BaO excitation spectrum for the Ba+O_2 reaction. The spectral region shown is the same as in Fig. 2, and the same operating conditions were used. No lines are marked since most cannot be identified. (See text).

It is found that the $v''=0$ rotational distribution can be fit moderately well with a Boltzmann distribution. A value for the rotational temperature of $T_{rot}=2000 \pm 300$ °K is obtained, where the error estimate is derived from the estimated experimental uncertainties in the fluorescence intensity. The simulated spectrum for a region centered about the (4, 0) band head using $T_{rot}=2000$ °K, as well as the derived rotational population distribution, is presented in Fig. 5. The representation of the true distribution by a Boltzmann form has the necessary shortcoming that such a form has a high-energy tail which extends beyond the exoergicity limit.

Rather than assuming some functional form for the rotational population distribution, we choose to determine a numerical distribution by fitting the data (peak heights above the fluorescence background) in a least-squares manner with appropriate constraints to a calculated spectrum. In the least-squares analysis, we allow the population of every 10th J value to vary freely with the constraint that the other populations be determined by linear interpolation. In addition, we constrain the end points by forcing the low J populations to be proportional to $2J+1$ (see Appendix A) and by terminating the high J populations at the exoergicity limit.[22]

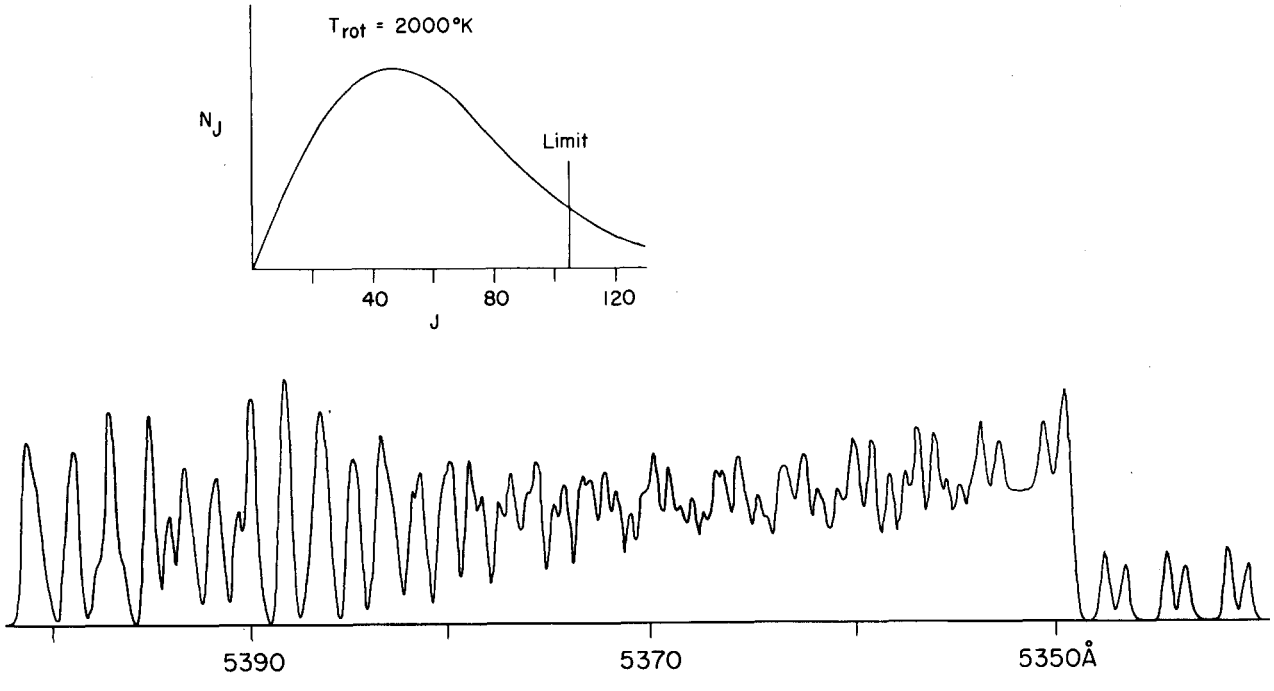

FIG. 5. Simulated BaO spectrum for the reaction Ba+CO_2 in the region about the (4, 0) head (see Fig. 1). A Gaussian bandwidth function with the experimental FWHM has been convoluted with the (4, 0) and (5, 0) line positions. A 2000 °K rotational distribution was assumed, and the limit marked in the rotational distribution shows the maximum J value energetically allowed for the $v=0$ level.

The free parameters are then determined in a least-squares manner[23] by minimizing the squares of the deviations between the experimental and calculated intensities at given wavelengths in the excitation spectrum.

Figure 6 presents the derived $v'' = 0$ rotational distribution for the $Ba + CO_2$ reaction, obtained from the least-squares fit of the (5, 0) band. For this distribution the average deviation between the experimental and calculated excitation spectra is 15% for 110 points (wavelengths). The form of this distribution is not smooth; the possible reasons for this behavior may be (1) the uncertainties in the experimental fluorescence intensities, (2) underlying spectral features from bands not included in the analysis, (3) the inadequacy of the assumed laser bandwidth function, (4) the inadequacy of the assumed interpolation between J populations, or (5) the preferential population of certain rotational levels by the reaction. Nevertheless, the derived distribution shows a falloff at high J levels which cannot be reproduced by a Boltzmann form. We note that the $v'' = 1$ and 2 rotational distributions are similar in shape to that presented in Fig. 6.

The vibrational populations may be obtained by comparing the intensities of different bands once the rotational distribution as a function of v'' is known. From an analysis of the (1, 0), (2, 0), (1, 1), (2, 1), (3, 1), (2, 2), and (4, 2) bands, we obtain $N_0 : N_1 : N_2 = 1.0 : 0.5 \pm 0.2 : 0.2 \pm 0.1$. If the vibrational populations are fit to a temperature T_{vib}, then a value of $T_{vib} = 1300 \pm 400$ °K is obtained.

B. The $Ba + O_2$ reaction

The difference in appearance and complexity of the BaO spectra between the $Ba + O_2$ and $Ba + CO_2$ reactions is startling. In the former reaction, all band heads in the BaO spectrum, part of which is shown in Figs. 3 and 4, are almost entirely missing, indicating that the populations of states of low J are very small. (Recall that the band head forms at $J \approx 5$.) Also the density of rotational lines is much greater, indicating that more v'' levels are significantly populated. Most of these lines cannot be identified since they arise from high (v', J') levels, for which high-resolution studies have not been carried out. Because of the electronic perturbations in the BaO $A\,^1\Sigma^+$ state, it is not prudent to extrapolate from the known line positions. The analysis by Field[19] of the perturbations in the $A-X$ system shows that the $a\,^3\Pi$ and $A'\,^1\Pi$ states are responsible for these perturbations and, moreover, the $a-X$ and $A'-X$ band systems are expected to occur in roughly the same spectral region as $A-X$. However, the unidentified lines in the present BaO excitation spectrum are almost certainly from the A state since a boxcar gate width of 1 μsec was used. The A' state has recently been observed in emission[24]; its lifetime has been measured by laser-induced fluorescence to be 9 ± 1 μsec.[25] The $a\,^3\Pi$ state is expected to have an even longer lifetime. Thus, the short gate width combined with the weakness of the $A'-X$ and $a-X$ transitions tends to discriminate against observation of the a and A' state fluorescence.

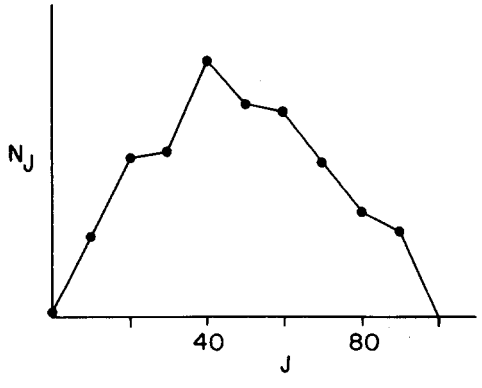

FIG. 6. The rotational distribution for the $v = 0$ BaO molecules formed from $Ba + CO_2$. The relative populations are derived by a least-squares fit of the rotational populations to the experimental spectrum. (See text).

As with the $Ba + CO_2$ reaction, we use the (4, 0) and (5, 0) bands to deduce the $v'' = 0$ rotational distribution. For these bands it is possible to identify lines for $40 \leq J'' \leq 110$. While the available reaction exoergicity allows levels up to $J'' \approx 140$ to be populated (see next section), it is difficult to identify such lines because of the lack of spectroscopic data. Thus it is not possible to determine relative populations of individual J'' levels or to use the convolution procedure described for $Ba + CO_2$ because of the presence of overlapping unidentified lines. Nevertheless we may partially characterize the rotational distribution from other considerations. For example, it is clear that the distribution is not Boltzmann in nature since T_{rot} would have to be about 10^4 °K to account for the almost complete absence of band heads. For a distribution of such a high T_{rot}, approximately 40% of the molecules would have $J'' > 140$ and this is not allowed from energy considerations. Although the band heads are weak, it can be seen from Fig. 3 that there is an increase in the baseline of the fluorescence intensity, best estimated by the intensity minima, starting at ~ 5350 Å and going to the red. This onset represents the start of the (4, 0) band. Since the $J'' = 0$ to 25 lines of the (4, 0) band occur within ~ 10 Å of the head and since the lines in this region that belong to the (5, 0) band have a J'' value of ~ 90, we may take the ratio of the (5, 0) to the (4, 0) features to be a measure of the population ratio

$$R = N_{90} \Big/ \sum_{J=0}^{25} N_J ,$$

since the rotational populations of the high J'' levels about $J'' = 90$ do not vary rapidly with J''. As before, we assume N_J is proportional to $2J+1$ for low J. By comparison of the experimental spectrum with simulated spectra we find that $R = 0.23 \pm 0.03$. It is interesting to note that if the proportionality between N_J and $2J+1$ holds to J values as high as 90, then $R = 0.268$.

Even though lines for $J'' > 110$ cannot be assigned, it is still possible to get information about the populations of very high J'' levels. As seen in Fig. 7, the intensities of the (5, 0) lines to the blue of the (4, 0) head show fluctuations much larger than the expected statistical variations; data from $Ba + CO_2$ have been included

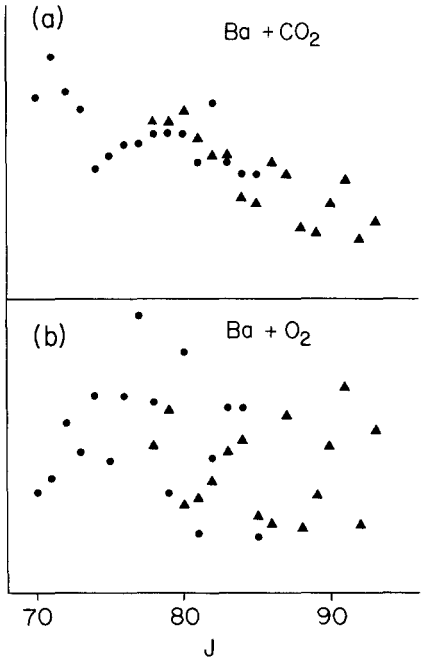

FIG. 7. Comparison of resolved rotational line peak intensities (experimental data) for the BaO (5, 0) band from the reactions (a) Ba + CO_2 and (b) Ba + O_2. The $R(J'')$ and $P(J'')$ lines are denoted by triangles and circles, respectively. In (b), the presence of bands other than (5, 0) is obvious from the large variation in peak intensities. The spectra were taken under the same conditions as Figs. 1 and 3.

for comparison. Moreover, even in this spectral region, there are some unassigned "extra" lines. Accordingly, we are led to the conclusion that other bands have significant intensity here. The most likely candidate is the (6, 0) band, for which the Franck–Condon factor[15] is 0.135 [compared to 0.165 and 0.161 for the (4, 0) and (5, 0) bands, respectively]. The J values would lie in the range 120 to 130. Other possible bands which may have significant intensity in this region are the (7, 1) and (8, 1) bands, but these would be expected to be about a factor of 2 weaker than the (6, 0) band. Figure 8 shows computer-generated spectra of the (4, 0) and (5, 0) bands with [Fig. 8(a)] and without [Fig. 8(b)] the (6, 0) band. Since spectroscopic information on the $v' = 6$ level is lacking, no perturbations were assumed and B_6' was obtained from the derived values for B_e' and α_e' of Field, English, Tanaka, Harris, and Jennings.[21] The spectrum in Fig. 8(b) shows a clear onset at the (4, 0) band head, while that in Fig. 8(a) and the experimental spectrum in Fig. 4 strongly suggests the presence of the (6, 0) band. With this assumption, we calculate the population ratio of (5, 0) to (6, 0) lines from the intensity fluctuations seen in the experimental spectrum [Fig. 7(b)]. We find the population ratio N_{125}/N_{90} to be 1 ± 0.3, where we have neglected the contribution from other overlapping bands. [Note from Fig. 8 that the (6, 0) $R(125)$ line is close in wavelength to the (5.0) $R(90)$ line]. Our deductions about the $v'' = 0$ rotational distribution are summarized in Fig. 9. A dotted line has been drawn to indicate the probable rotational distribution. From the close resemblance of the $v'' = 0$ and $v'' \neq 0$ band contours, the rotational distributions are similar for all the v'' levels observed ($v'' = 0$ to 3). (Note that the energy limit varies from $J'' = 139$ at $v'' = 0$ to $J'' = 114$ at $v'' = 3$.)

We are not able to obtain the vibrational distribution from the low-pressure spectra. At higher O_2 pressures, band heads appear because of collisional relaxation of the rotational distribution. We can use the height of these band heads as a measure of the vibrational band intensities and hence vibrational population, if several reasonable assumptions are made: (1) there is no collisional vibrational relaxation; (2) the rotational distributions do not vary much with v''; and (3) rotational relaxation is the same in all v'' levels. Using data taken at an O_2 pressure of $\sim 8 \times 10^{-4}$ torr (approximately

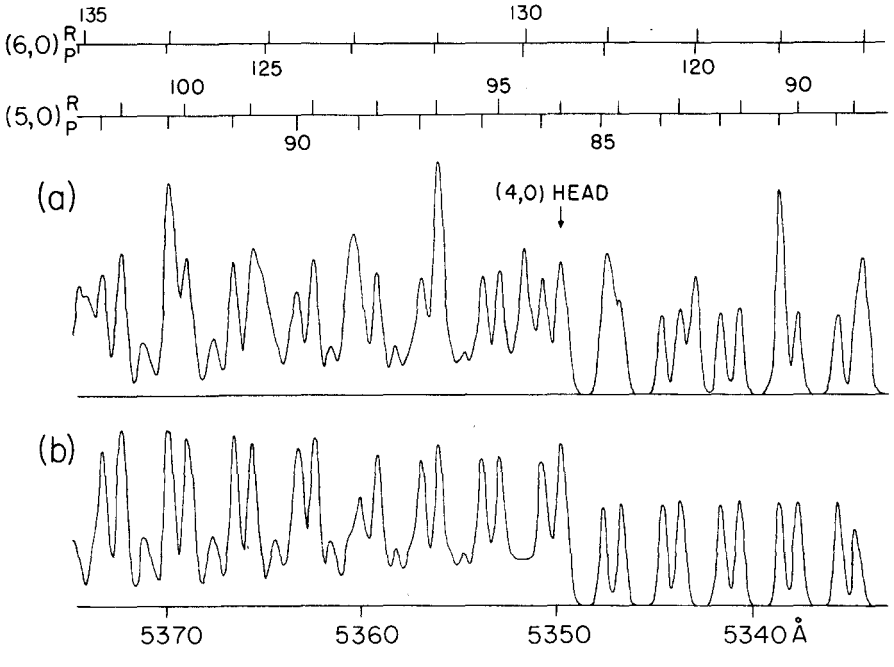

FIG. 8. Simulated spectra using the derived $v = 0$ BaO rotational distribution for the Ba + O_2 reaction. In (a), the (4, 0), (5, 0) and (6, 0) bands are included; in (b), only the (4, 0) and (5, 0) bands are included.

a factor of 10 higher than in the low-pressure scans), we find $N_0 : N_1 : N_2 : N_3 : N_4 = 1.0 : 0.7 : 0.7 : 0.6 : 0.6$. The experimental uncertainties in these ratios are on the order of 0.2. No information about higher v'' levels could be obtained.

C. Reaction energies: Determination of D_0^0(BaO)

From the Ba + CO_2 reaction it is possible to set a lower bound to the BaO dissociation energy, D_0^0(BaO), by identifying the highest rotational level J_{max} of the $v = 0$ level populated in the reaction. (For simplicity we omit from here on double primes to designate ground state quantum numbers.) From a knowledge of D_0^0(CO–O) = 125.7 ± 0.1 kcal/mole[26] and an estimate of the thermal energy of the reactants, we can obtain from energy conservation a lower bound.

$$D_0^0(\mathrm{BaO}) \geq D_0^0(\mathrm{CO{-}O}) + B_0 J_{max}(J_{max}+1) - E_{trans}^i - E_{int}(\mathrm{CO_2}) , \quad (3)$$

where E_{trans}^i is the average translational energy of the reactants (in the center-of-mass system) and $E_{int}(CO_2)$ is the average internal energy of CO_2. The value of D_0^0(BaO) given by Eq. (3) is a lower bound because the internal energy of the product CO, E_{int}(CO), and the relative translational energy of the products, E_{trans}^f, have been neglected.

Figure 1 shows the presence of the (5, 0) R(95) line, and hence the highest J level observed is 95. It is likely that even higher J levels are produced in this reaction, although with decreasing populations. In Fig. 10 we have plotted the individual intensities of resolved rotational lines in the (5, 0) band as a function of J. As can be seen from Eq. (2), these intensities are proportional to populations. A linear extrapolation of the intensities as a function of J yields the limit $J_{max} = 105 \pm 4$. The value is also consistent with an extrapolation using Fig. 7(a).

We calculate[27] E_{trans}^i by taking a 90° intersection angle between the most probable velocities v_{mp} of the reactants. The Ba beam is assumed to be effusive, so that $v_{mp}(\mathrm{Ba}) = [3RT(\mathrm{Ba})/m(\mathrm{Ba})]^{1/2}$, while the velocity of CO_2 gas inside a volume is given by $v_{mp}(\mathrm{CO_2}) = [2RT(\mathrm{CO_2})/m(\mathrm{CO_2})]^{1/2}$. We find $E_{trans}^i = 1.67$ kcal/mole. We also find $E_{int}(\mathrm{CO_2}) = E_{rot}(\mathrm{CO_2}) + E_{vib}(\mathrm{CO_2}) = 0.73$ kcal/mole, where $E_{rot}(\mathrm{CO_2}) = RT(\mathrm{CO_2})$ and $E_{vib}(\mathrm{CO_2}) = R\sum_i d_i \Theta_i / [\exp(\Theta_i/T) - 1]$, and i is summed over the 3 vibrational modes. Here d_i is the degeneracy of mode i; and $\Theta_i = \hbar\omega_i/k$, where ω_i is the frequency.[28] Then from Eq. (3) we find $D_0^0(\mathrm{BaO}) \geq 133.5 \pm 1.3$ kcal/mole, where the error estimate includes the uncertainty in the J_{max} value and the probable spread in E_{trans}^i (taken to be ±1 kcal/mole).

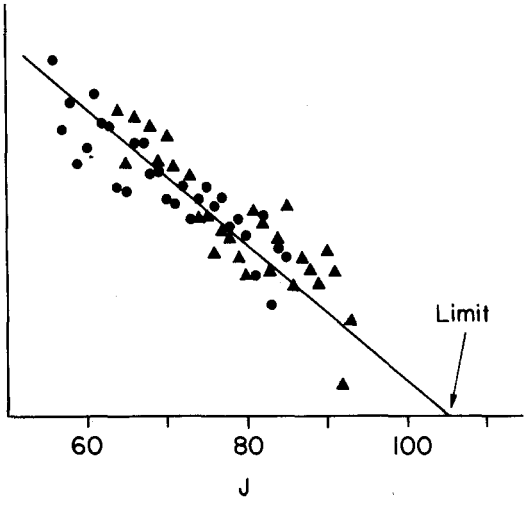

FIG. 10. Resolved rotational line peak intensities (experimental data) for the (5, 0) band from Ba + CO_2. The solid line shows the extrapolation used to obtain the maximum J value energetically allowed in this reaction. The $R(J'')$ and $P(J'')$ lines are denoted by triangles and circles, respectively. The spectrum was taken under the same conditions as Fig. 2.

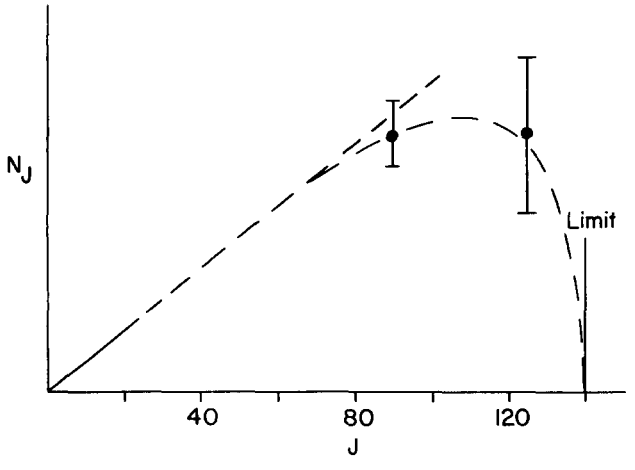

FIG. 9. The derived rotational distribution for the $v = 0$ BaO molecules formed from Ba + O_2. The maximum J level energetically allowed has been indicated. A dotted curve shows the likely shape of the distribution. (See text).

We believe this lower bound is actually an equality to within the stated error. The method of extrapolation compensates for the neglect of E_{int}(CO) and E_{trans}^f by assuming that the rotational populations vs J are well represented by a linear function near the exoergicity limit. A justification for this assumption is that a phase space calculation for the reaction Ba + CO_2 displays this behavior (see Sec. IVB). Consequently, we conclude that

$$D_0^0(\mathrm{BaO}) = 133.5 \pm 1.3 \text{ kcal/mole} . \quad (4)$$

It is reassuring that a previous study[29] yielded the lower limit $D_0^0(\mathrm{BaO}) \geq 131.5$ kcal/mole, based on the observation of the highest BaO* state populated in the chemiluminescent reaction Ba + NO_2. It is also encouraging to note that dissociation energies derived from chemiluminescence and laser-induced fluorescence studies have been found to be in substantial agreement for the case of D_0^0(AlO) as well.[27]

Using the value of D_0^0(BaO) given in Eq. (4), we present in Table I a summary of the energetics for the Ba + O_2 and Ba + CO_2 reactions. Here, E_{tot} and E_{tot}' denote, respectively, the total energy of the reactants and the products. The spread in the product energy E_{tot}' caused

TABLE I. Summary of reaction energetics (energies in kcal/mole).[a]

	$Ba + O_2$	$Ba + CO_2$
I. Reactants		
E_{vib}	~0	0.15
E_{rot}	0.58	0.58
E^{l}_{trans}	1.15	1.67
E_{tot}	1.73	2.40
II. Products		
E'_{tot}	17.2	10.2
v_{max}	9	5
$J_{max}(v=0)$	139	105

[a]The reactant energies are calculated as described in the text for $Ba + CO_2$. The dissociation energies D^0_0 $(O_2) = 117.97 \pm 0.1$ kcal/mole and D^0_0 $(CO-O) = 125.7 \pm 0.1$ kcal/mole are taken from Ref. 26.

by the thermal spread in the reactant energy is a small fraction of E'_{tot} because the exothermicity of both reactions is large compared to E_{tot}. Hence, comparison of the experimental internal state distributions with theoretically calculated ones does not require thermal averaging of the calculated distributions. The last two rows of Table I show the highest vibrational level v_{max} and the highest level J_{max} (in $v=0$) of BaO which are energetically accessible in each reaction. It is obvious from this table that the $Ba + O_2$ reaction can populate higher v and J levels than $Ba + CO_2$. It is this fact which has greatly hindered the analysis of the $Ba + O_2$ excitation spectrum.

IV. DISCUSSION OF INTERNAL STATE DISTRIBUTIONS

A. Gross features

The present results on the $Ba + O_2$ reaction show that at least two-thirds of the available energy E'_{tot} appears as BaO internal excitation. The most striking feature is the amount of energy found in product rotation. Fully one-half of E'_{tot} is funneled into rotation for molecules produced in the $v=0$ level, and we estimate that about one-third of E'_{tot} results in rotation when all v levels are considered. The preliminary report[1] on $Ba + O_2$ considerably underestimated the amount of BaO rotational excitation because of the efficient collisional rotational relaxation of BaO by the O_2 gas in the scattering chamber. We may estimate an average rotational relaxation cross section σ from a knowledge of the density n of O_2 at which relaxation of BaO becomes evident in the excitation spectrum. Taking n equal to 3×10^{12} molecules/cm^3 (10^{-4} torr), and taking an upper limit to the path length l of the gas to be 6 cm (the distance from the bulkhead flange between the oven and scattering chambers to the laser excitation zone), we find $\sigma \geq 50$ Å^2. Here we have set $n\sigma l$ equal to 0.1 as the limit to observability of relaxation in the excitation spectrum. This value for σ is a lower limit since we have assumed all BaO molecules are fomed at the bulkhead flange and travel a distance l before being detected. The large magnitude of σ is indicative of the large BaO dipole moment[20] ($\mu_0 = 7.954$ D) which allows efficient rotational relaxation. Comparison of the present vibrational distribution with that previously reported suggests that the early experiments may have also suffered some vibrational relaxation. However, the probable errors in the present distribution are quite large. The average vibrational energy is on the order of one-third of E'_{tot}, as previously suggested.[1]

A caveat must be included with all our deductions about the BaO internal state distribution. Laser-induced fluorescence measures the density of molecules in a particular (v, J) state. However, cross sections are related to fluxes. In the previously studied reaction systems,[11] all the molecules had about the same laboratory velocity $\mathbf{v}_{lab}$, and the conversion of densities to fluxes was trivial. However, for the present reactions, the BaO laboratory velocities $\mathbf{v}_{lab}$ may vary greatly with (v, J) state since the center-of-mass velocity of BaO is comparable to $\mathbf{v}_{cm}$, the velocity of the center-of-mass. For $Ba + O_2$, however, we may use the angular distribution data of Loesch and Herschbach[4] to set limits on the variation of $\mathbf{v}_{lab}$. Since they find the total BaO distribution peaks at 0° and 180° and that both peaks have about equal intensity. It is found that $\mathbf{v}_{lab}$ decreases by about 6% as v goes from 0 to 8 for $J=0$. Similarly, for $v=0$ the same estimate obtains as J goes from 0 to 120. The actual variation of $\mathbf{v}_{lab}$ could be greater but is probably not significantly larger than our 10–20% experimental uncertainties. Finally, we note that if BaO from $Ba + CO_2$ is also assumed to scatter entirely to 0° and 180°, then possible variation of $\mathbf{v}_{lab}$ is about identical to that for $Ba + O_2$.

The present results on the BaO product state distribution can be improved considerably. For $Ba + O_2$, we have succeeded only in obtaining the qualitative shape of the $v=0$ rotational distribution and a very rough vibrational distribution. The $Ba + O_2$ excitation spectrum has turned out to be a pathological case for product state analysis by the method of laser-induced fluorescence because very high rotational levels are populated and the A state perturbations prevent extrapolation to the high (v, J) line positions, for which high resolution spectroscopic data are lacking. The analysis of the spectrum would be greatly aided by further spectroscopic study of the BaO $A-X$ system. Furthermore, the facile BaO rotational relaxation puts a premium on efficient signal collection because of the low pressures of reagent gas required. The problem of small signals is compounded by the fact that the BaO spectrum spreads over ~2000 Å, and hence scans over large spectral regions are required. Nevertheless, the present results on $Ba + O_2$ provide useful information complementary to the molecular beam results. The $Ba + CO_2$ spectrum is simpler, and hence we have obtained more quantitative data on this BaO distribution. However, we can look forward to refinements in the product state analysis of both reactions in the future.

B. Comparison of phase space and transition state theories with experiment

Loesch and Herschbach,[4] based on their angular and recoil velocity distributions, have concluded that the $Ba + O_2$ reaction proceeds through a long-lived complex and that the available energy is partitioned among the various modes "statistically." Accordingly, these findings have led us to compare the experimentally determined BaO internal state distributions for both $Ba + O_2$ and $Ba + CO_2$ with two statistical models.

In the quantum mechanical formulation of phase space theory,[30] it is assumed that the dissociation of the collision complex depends only on the dynamical quantities (energy, total angular momentum, and its projection) conserved in the complex and not on the initial state from which the complex is formed. Moreover, the probability of breakup of the complex to any state of given energy and angular momentum is assumed to be *a priori* equal. Consequently, phase space theory merely requires one to count the number of states accessible to the complex under the conservation of total energy and angular momentum. Even for reactions with no activation energy, the existence of centrifugal barriers in the entrance and exit channels limits the number of states accessible and causes the internal state distribution to differ to some extent from a Boltzmann distribution, as would be the (unphysical) case for no barriers.

We have assumed that the reactions $Ba + O_2$ and $Ba + CO_2$ do not have activation barriers and that the long-range part of their interaction potentials is governed by a van der Waals term of the form $V(r) = -C^{(6)}r^{-6}$ for both the entrance and exit channels. The $C^{(6)}$ constants are estimated as the sum of a Slater–Kirkwood dispersion term[31] (induced dipole–induced dipole) and an induction term[32] (dipole–induced dipole), and the results are listed in Table II. The Keesom alignment term[33] (dipole–dipole) for the exit channel $BaO + CO$ is neglected because of the small magnitude of the CO dipole moment. For a 3-atom complex ($Ba + O_2$), internal state distributions are calculated using Eq. (6b) of Pechukas, Light, and Rankin[30]; for a 4-atom complex ($Ba + CO_2$), an extension of the formalism of Pechukas *et al.* is developed (see Appendix A) and applied. The reactants O_2 and CO_2 are treated as $^1\Sigma^+$ molecules with no nuclear spin statistics; this approximation is justified for these calculations because the number of reactant states accessible to the complex is small compared to that of the product states so that the total number of accessible states for a complex at a given energy and angular momentum is negligibly overestimated. For both systems, the reactants are assumed to be in their lowest internal states, and the initial relative translational energies are set equal to the values of E_{tot} in Table I. It is found that the calculated internal states distributions are insignificantly altered if, instead, the most probable J values for 300 °K O_2 and CO_2 are used with a corresponding decrease in the relative tranlational energy. We have used the value of $D_0^0(BaO)$ given in Eq. (4) to calculate reaction exothermicities. Finally, we note that we have made the additional assumption that $Ba + O_2$ and $Ba + CO_2$ react only to yield neutral products.[34]

TABLE II. Potential parameters and van der Waals constants used in the statisitical theories.

	α (Å^3)	μ(D)	$C^{(6)}$(10^{-60} erg − cm^6)
	A. $Ba + O_2 \rightarrow BaO + O$		
Reactants			353
Ba	43.6[a]		
O_2	1.62[b]		
Products			138
BaO	5.5[c]	7.954[d]	
O	0.77[b]		
	B. $Ba + CO_2 \rightarrow BaO + CO$		
Reactants			573
Ba	43.6[a]		
CO_2	2.65[e]		
Products			335
BaO	5.5[c]	7.954[d]	
CO	1.95[e]	0.112[f]	

[a]S. A. Adelman and A. Szabo, J. Chem. Phys. 58, 687 (1973).
[b]R. A. Alpher and D. R. White, Phys. Fluids 2, 153 (1959).
[c]The sum of the ionic polarizabilities. J. H. Van Vleck, *The Theory of Electric and Magnetic Susceptibilities* (Oxford U. P., London, 1932).
[d]Value of μ_0. Reference 20.
[e]Reference 31, p. 950.
[f]C. A. Burrus, J. Chem. Phys. 28, 427 (1958).

Figure 11 presents the BaO product vibrational distributions calculated by phase space theory. For $Ba + CO_2$, the rapid falloff of vibrational population with increasing v matches rather closely the observed population ratios. The more gradual falloff from the reaction $Ba + O_2$ also agrees within the large experimental uncertainties with observation. It should be noted that the calculated vibrational distribution for $Ba + CO_2$ is well characterized by a temperature, whereas the distribution for $Ba + O_2$ falls off too slowly to be described satisfactorily by a vibrational temperature. This nonthermal distribution from a statistical theory happens quite often for complexes having few degrees of freedom, which cannot be regarded as infinite "heat baths." This fact becomes even more striking when we consider rotational distributions.

Figures 12(a) and 12(b) illustrate the phase space calculations of the relative rotational populations for $v = 0$ BaO molecules formed by $Ba + CO_2$ and $Ba + O_2$, respectively. Comparison of Fig. 12(a) with the experimentally derived distribution in Fig. 6 for $Ba + CO_2$ and comparison of Fig. 12(b) with Fig. 9 for $Ba + O_2$ show that phase space calculations are in rather remarkable agreement with experiment. As mentioned previously, the phase space calculations show that the relative rotational populations for low J values are proportional to $2J + 1$, and this behavior is shown in Appendix A to be rather general. The distributions in both Figs. 12(a) and 12(b) cannot be characterized by a rotational temperature. This is particularly pronounced for the reaction $Ba + O_2$ and helps to explain the lack of band heads in the experimental excitation spectrum.

We conclude that the BaO internal state distributions for both the reactions $Ba + O_2$ and $Ba + CO_2$ follow closely the predictions of phase space calculations. Moreover,

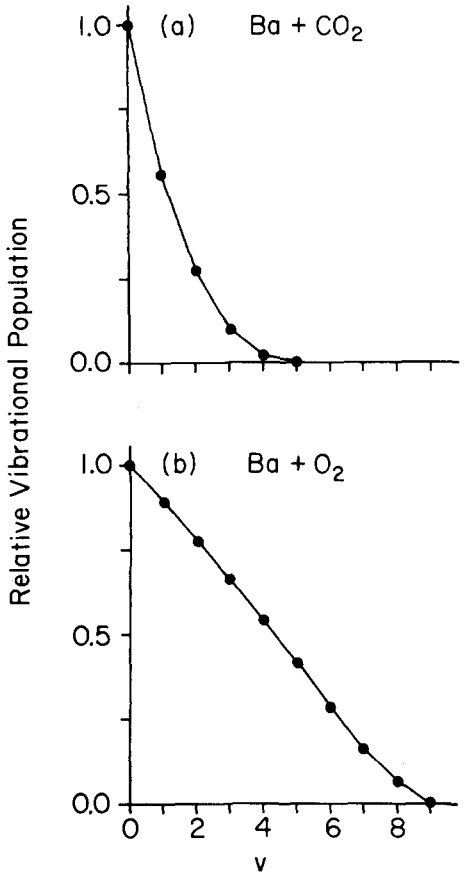

FIG. 11. Phase space calculations of the relative BaO vibrational populations as a function of v for the reactions (a) $Ba + CO_2$ and (b) $Ba + O_2$. The populations are normalized so that the value of the most populated level is unity. The points are connected by straight-line segments for clarity.

the BaO internal state distribution from $Ba + O_2$ is consistent with the interpretation of Loesch and Herschbach[4] that this reaction proceeds through a persistent complex. While no molecular beam study of $Ba + CO_2$ has been reported, our results strongly suggest that it also involves a persistent complex. It must be realized, however, that phase space theory does not make any assumptions about the lifetime of the collision complex. Although neither angular distribution studies nor internal state distribution studies, taken alone, can provide a complete picture of the reaction dynamics, we are very fortunate here to be able to use the data of Loesch and Herschbach to sharpen our understanding of these reactions.

Another statistical model which has enjoyed considerable success for the calculation of product translational energy distributions resulting from the decay of collision complexes formed in bimolecular reactions is the transition state theory of Safron, Weinstein, Herschbach, and Tully.[35] This model is inspired by the RRKM theory of unimolecular decomposition[36] and, as in the phase space theory, the reactions are assumed to have no activation barriers but rather centrifugal barriers in the entrance and exit channels. In addition, the calculations are simplified by assuming that (1) the initial and final orbital angular momenta equal the total angular momentum (the internal angular momenta are assumed to be negligible) and (2) the rate of dissociation of the complex into the products need not be normalized for dissociation of the complex back to the reactants.

Safron has presented formulas in his thesis[37] for the internal state distributions for 3-atom complexes, using classical energy level densities (see Appendix B). We have extended his treatment in Appendix B to 4-atom complexes. Two major types of complexes may be distinguished: (1) a "loose" complex, in which the subunits (incipient products) are free to rotate; and (2) a "tight" complex, in which the free rotations of the subunits are considered to be bending modes of the complex. In addition, "tight" complexes may be subdivided into "linear" and "nonlinear", depending on their geometry. As Marcus[38] has pointed out, "tight" complexes imply that there are strong interactions between the incipient products as the complex breaks up. In the present treatment, it is assumed that the modes of the complex can be put into a one-to-one correspondence with the modes of the products.

Using the van der Waals constants listed in Table II, we have applied this transition state theory to calculate the relative rotational populations of BaO products in the $v = 0$ level for $Ba + CO_2$ [Fig. 12(c)] and $Ba + O_2$ [Fig. 12(d)]. These calculations have been performed for $Ba + O_2$ using a "loose" complex (solid line) and "tight" linear (dot-dashed line) and nonlinear (dashed line) complexes; for $Ba + CO_2$ a "loose" complex (solid line), a "tight" linear complex (dot-dashed line), and a "tight" nonlinear complex with two different allocations of the modes of the complex between incipient BaO and CO (dashed and dotted lines) are calculated. Comparison of transition state theory with phase space theory calculations shows that in all cases the two statistical theories yield significantly different distributions. The "tight" complexes fail to show the correct low J dependence, while the "loose" complexes fall too rapidly at high J. Safron *et al.*[35] have claimed that their transition state theory for a "loose" complex can be derived with equivalent assumptions from phase space theory. Nevertheless we find significant differences between the phase space theory and the "loose" complex transition state theory calculations for the present reactions. Possible sources for these differing results are assumptions (1) and (2) made by Safron *et al.* in their transition state theory but which were not made in the phase space theory. Since the present reactions are fairly exothermic, assumption (2) concerning back reaction is well satisfied, while assumption (1) concerning the relative magnitudes of the initial and final orbital angular momenta is suspect.

It is to be emphasized that the transition state theory of Safron *et al.* was not developed primarily for the calculation of detailed internal state distributions. Moreover, it is striking how well this simple theory reproduces the gross features of the experimental distribution, as well as those of the phase space theory. Nonetheless, these calculations indicate that some future modifications of the transition state theory will be required to predict detailed internal state distributions, at least for complexes with few degrees of freedom.

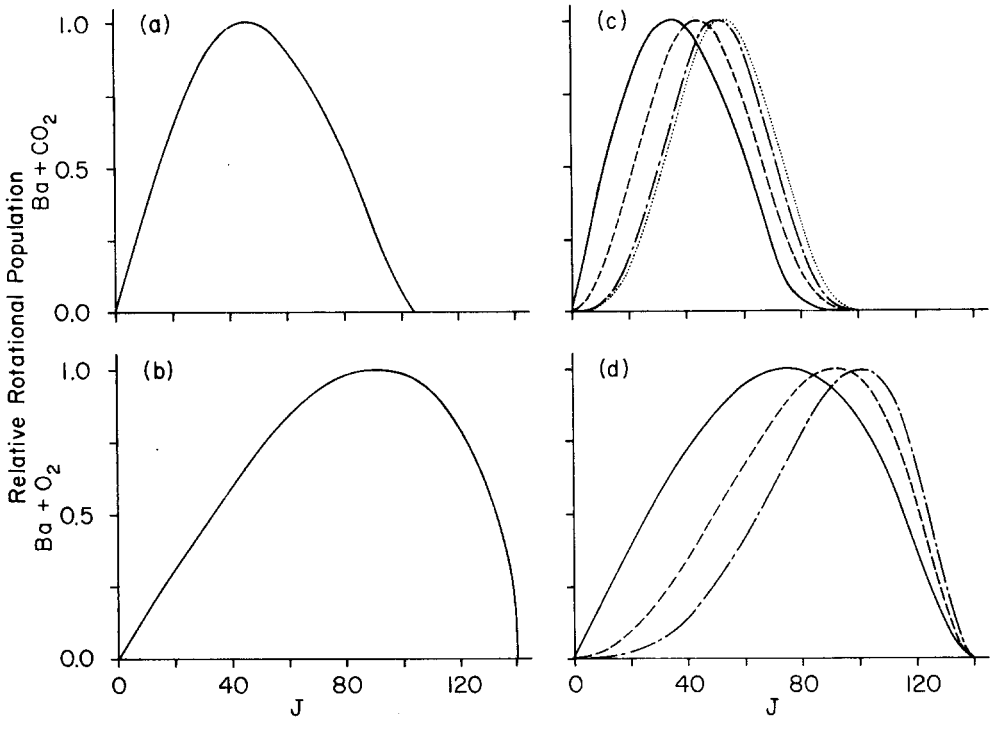

FIG. 12. Comparison of relative rotational populations predicted by phase space theory (PST) and transition state theory (TST). Shown are the $v=0$ BaO distributions for the reactions Ba + CO_2 [(a) PST and (c) TST] and Ba + O_2 [(b) PST and (d) TST]. In (c), the solid line represents the results for a "loose" complex, the dot-dashed line represents a "tight" linear complex, and the dashed and dotted lines represent, respectively, forms A and B of a "tight" nonlinear complex. (See text and Table III). In (d), the solid line represents the results for a "loose" complex, and the dot-dashed and dashed lines represent a "tight" linear and a "tight" nonlinear complex, respectively.

ACKNOWLEDGMENTS

We thank D. R. Herschbach for making the Ba + O_2 angular distribution data available to us prior to publication and for pointing out to us the expected nonthermal nature of the distributions calculated from transition state theory for complexes having few degrees of freedom. We were greatly aided by R. Couppez, J. G. Pruett, and R. K. Sander who rf shielded the Molectron nitrogen laser. We are also grateful to Diane L. Feldman who helped write the computer programs used for the phase space theory calculations, to P. Pechukas for many useful discussions concerning phase space theory, and to S. Safron, R. D. Levine, and R. A. Marcus for comments concerning transition state theory. Support of this work by the Advanced Research Projects Agency of the Department of Defense monitored by the U. S. Army Research Office, Durham, under Grant DA-ARO-D-31-124-70-G103; by the U. S. Army Research Office, Durham, under Grant DA-ARO-D-31-124-73-G147; and by the Air Force Office of Scientific Research under Grant AFOSR-73-2551A is gratefully acknowledged.

APPENDIX A. PHASE SPACE THEORY

We first summarize the results obtained by Pechukas, Light, and Rankin[30] for a 3-atom complex; then we extend their treatment to a 4-atom complex. Finally we prove that the cross section is proportional to $2J+1$ for low J. We follow the notation of Pechukas *et al.*

For the reaction A + BC → AB + C, the cross section $\sigma(n_f, M_f, E_f; n_i, M_i, E_i)$ for formation of product molecules in a final vibration–rotation level (n_f, M_f) with a final relative translational energy E_f from reactants in an initial (n_i, M_i) level at an initial relative translational energy $E_i = E_f - Q_{fi}$, where Q_{fi} is the exothermicity, is given by Eq. (6b) of Pechukas *et al.*:

$$\sigma(n_f, M_f, E_f; n_i, M_i, E_i) = \frac{\pi\hbar^2}{2\mu_i E_i (2M_i+1)} \sum_{L_i=0}^{L_{i\max}} \sum_{|L_i - M_i| \le K \le (L_i + M_i)} (2K+1) \sum_{L_f} P(n_f, M_f, L_f, E_f; E_T, K, K_z) \,. \tag{A1}$$

Four-atom complex

Now consider the 4-atom reaction

$$A + BCD \rightarrow AB + CD. \tag{A2}$$

Let the subscripts i, $f1$, and $f2$ denote, respectively, the molecules BCD, AB, and CD, and let n_i denote the set (v_1, v_2^l, v_3) which specifies the vibrational level of BCD, assumed to be a linear molecule. Then in a derivation entirely analogous to Eq. (A1), we find

$$\sigma(n_{f1}, M_{f1}, n_{f2}, M_{f2}, E_f; n_i, M_i, E_i) = \frac{\pi\hbar^2}{2\mu_i E_i(2M_i+1)} \sum_{L_i=0}^{L_{i\max}} \sum_{|L_i - M_i| \le K \le (L_i + M_i)} (2K+1) \sum_{Lf} P(n_{f1}, M_{f1}, n_{f2}, M_{f2}, L_f, E_f; E_T, K, K_z) . \tag{A3}$$

The internal state distribution for molecule AB is then obtained by summing over the possible states of CD for a given state of AB:

$$\sigma(n_{f1}, M_{f1}; n_i, M_i, E_i) = \sum_{n_{f2}} \sum_{M_{f2}} \sigma(n_{f1}, M_{f1}, n_{f2}, M_{f2}, E_f; n_i, M_i, E_i) . \tag{A4}$$

The evaluation of the probability $P(n_{f1}, M_{f1}, n_{f2}, M_{f2}, L_f, E_f; E_T, K, K_z)$ that a 4-atom complex dissociates to a particular accessible state is considerably more tedious. As before, we have

$$P(n_{f1}, M_{f1}, n_{f2}, M_{f2}, L_f, E_f; E_T, K, K_z) = 1/N(E_T, K, K_z). \tag{A5}$$

However, the total number of accessible states $N(E_T, K, K_z)$ of the complex is now given by

$$N(E_T, K, K_z) = \sum_{n_i} \bar{n}(n_i; E_T, K, K_z) + \sum_{n_{f1}} \sum_{n_{f2}} \bar{n}(n_{f1}, n_{f2}; E_T, K, K_z). \tag{A6}$$

The terms in the sum over n_i in Eq. (A6) are computed in the same manner as Pechukas *et al.* (see their Fig. 1). The terms in the sums over n_{f1} and n_{f2} require a more complex algorithm for their evaluation. Figure 13 illustrates the computation of one term. Here $\bar{n}(n_{f1}, n_{f2}; E_T, K, K_z)$, which represents the number of states of the reaction products in the vibrational levels n_{f1} and n_{f2} accessible from (E_T, K, K_z), is the number of integer lattice points within or on the edge of the volume in (L_f, M_{f1}, M_{f2}) space defined by the relations

$$L_f(L_f+1)\hbar^2 \le 6\mu_f C_f^{1/3} [\tfrac{1}{2} E_f(n_{f1}, M_{f1}, n_{f2}, M_{f2})]^{2/3} , \tag{A7a}$$

$$|L_f - M_{12}| \le K \le (L_f + M_{12}) , \tag{A7b}$$

$$|M_{f1} - M_{f2}| \le M_{12} \le (M_{f1} + M_{f2}) . \tag{A7c}$$

Equations (A3) through (A7) give the prescription for calculating according to phase space theory the AB product state distribution for the reaction A + BCD → AB + CD. In the above, we treated the BCD as linear, but the generalization to a bent triatomic requires only taking account of the extra rotational degrees of freedom. The extension of phase space theory to complexes with 5 atoms or more is straightforward. However, the computational effort grows rapidly.

Low J behavior

Finally, we show that the cross section for formation of low M_f states is proportional to $2M_f + 1$ for a 3-atom complex. The sum over L_f in Eq. (A1) for low M_f is not restricted by the height of the centrifugal barrier [see Eq. (4b) of Ref. 30] since $L_{f\max}$ is usually large compared to K in an exothermic reaction. Moreover, K is greater than M_f for most terms in the sum over K in Eq. (A1) so that $M_f \ll K \ll L_{f\max}$. Then the angular momentum coupling restrictions [see Eq. (4a) of Ref. 30] allows the sum $\sum_{L_f} 1$ to be equated with $2M_f + 1$. Hence, we find for the 3-atom complex

$$\sigma(n_f, M_f, E_f; n_i, M_i, E_i) = k \sum_{L_i} \sum_{K} (2K+1) \sum_{Lf} P(n_f, M_f, L_f, E_f; E_T, K, K_z)$$

$$\approx k \sum_{L_i} \sum_{K} (2K+1)(2M_f+1) P(n_f, M_f, L_f, E_f; E_T, K, K_z)$$

$$= k'(2M_f+1), \tag{A8}$$

where k and k' are proportionality constants. The same considerations, when applied to a four-atom complex, lead to the same result. This conclusion that the cross section is proportional to $2J+1$ for low J values is not restricted[39] to phase space theory although it does require that many J levels of the products be accessible.

APPENDIX B. TRANSITION STATE THEORY

We review the calculation of rotational distributions using the transition state theory of Safron, Weinstein, Herschbach, and Tully.[35] The results for 3-atom complexes have been obtained previously by Safron in his thesis,[37] and we list them here for reference. Finally,

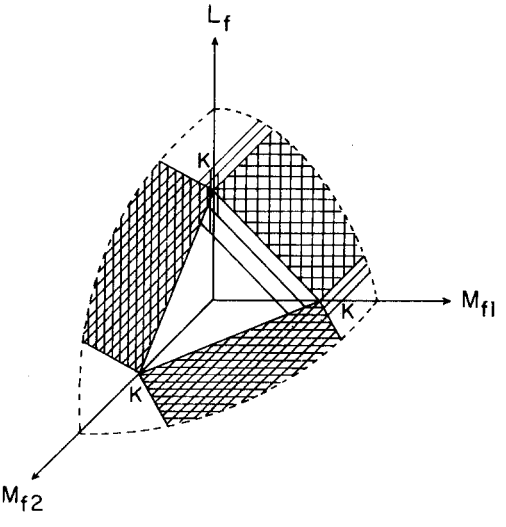

FIG. 13. Region of summation in (L_f, M_{f1}, M_{f2}) space for $\bar{n}(n_{f1}, n_{f2}; E_T, K, K_z)$ occurring in Eq. (A6). For clarity, some of the lattice points have been omitted. Note that for fixed M_{f2} the region of summation over the plane in (L_f, M_{f1}) space is, in general, a figure having five straight-line interior segments and a curve defining the exterior.

we extend the transition state theory to the calculation of rotational distributions of diatomic products from 4-atom complexes.

We follow the notation of Safron *et al.*, with some additions: we let W_r' be the product rotational energy, N_r be the energy level density of the transition state modes that become product rotation, and W_v^* be the total state function for those modes other than those in N_r and the reaction coordinate. With the assumptions of Safron *et al.*, the product rotational energy distribution for all molecules is given by

$$P_r(W_r') = kN_r(W_r') \int_0^a W_v^*(\mathcal{E}' - B' - W_r')\, P(B')dB' , \quad \text{(B1)}$$

where

$$a = B_m' \text{ if } W_r' \leq \mathcal{E}' - B_m',$$
$$= \mathcal{E}' - W_r' \text{ if } W_r' > \mathcal{E}' - B_m' ,$$

and k is a proportionality constant. The relative rotational populations are then

$$N_J = (2J+1)P_r(B\,J[J+1]) . \quad \text{(B2)}$$

Equation (B1) is similar to Eq. (V-57) in Safron's thesis.[37] For 3-atom complexes, it would appear that $P_r(W_r')$ represents the rotational energy distribution for molecules formed in the $v = 0$ level, as well. For 4-atom complexes, the $v = 0$ rotational energy distribution requires that W_v^* be replaced by W^* in Eq. (B1), where W^* is the total state function for modes other than those in N_r, the reaction coordinate, and the mode that becomes product vibration.

Let v and r denote, respectively, the number of vibrational modes excluding the reaction coordinate and the number of "active"[36] rotational modes at the transition state. These degrees of freedom are divided into two groups, those which become product rotation (N_r) and those which become other internal degrees of freedom of the products (W_v^*). Table III lists values of v and r and the partitioning of these modes between N_r and W_v^* for "tight" linear, "tight" nonlinear and "loose" 3-atom and 4-atom complexes. The partitioning between N_r and W_v^* for a 3-atom complex is unambiguous. However, the choices for a 4-atom complex is not as clear-cut. In all cases, the six degrees of freedom of the complex evolve into the vibrational modes of the diatomics (two modes) and two rotational modes of each diatomic (four modes in all). Since it is unlikely that rotational modes of the complex evolve into product vibration, two out of the v vibrational modes are allocated to W_r^*. This restriction fixes the allocation of modes for "tight" linear and "loose" complexes. However, as can be seen in Table III, there are two possible ways of dividing the modes for a "tight" nonlinear complex.

Explicit formulas for the rotational energy distributions from a 3-atom complex may be derived from Eq. (B1), using classical energy level densities.[40] With the help of Table III, we find:

1. "Tight" linear complex.

$$P_r(W_r') = kW_r'(\mathcal{E}' - W_r' - \tfrac{2}{5}B_m')B_m'^{2/3} \quad \text{for } W_r' \leq \mathcal{E}' - B_m'$$
$$= \tfrac{3}{5}kW_r'(\mathcal{E}' - W_r')^{5/3} \quad \text{for } W_r' > \mathcal{E}' - B_m'. \quad \text{(B3)}$$

TABLE III. Number of vibrational and "active" rotational degrees of freedom in the transition state.

Type of complex	Vibrations v	"Active" rotations r
3-atom complex		
"Tight" linear	3	0
Product rotation (N_r)	2	0
Other product modes (W_v^*)	1	0
"Tight" nonlinear	2	1
Product rotation (N_r)	1	1
Other product modes (W_v^*)	1	0
"Loose"	1	2
Product rotation (N_r)	0	2
Other product modes (W_v^*)	1	0
4-atom complex		
"Tight" linear	6	0
Product rotation (N_r)	2	0
Other product modes (W_v^*)	4	0
"Tight" nonlinear	5	1
Form *A*		
Product rotation (N_r)	1	1
Other product modes (W_v^*)	4	0
Form *B*		
Product rotation (N_r)	2	0
Other product modes (W_v^*)	3	1
"Loose"	2	4
Product rotation (N_r)	0	2
Other product modes (W_v^*)	2	2

2. "Tight" nonlinear complex.

$$P_r(W_r') = kW_r'^{1/2}(\mathcal{E}' - W_r' - \tfrac{2}{5}B_m')B_m'^{2/3} \quad \text{for } W_r' \leq \mathcal{E}' - B_m'$$
$$= \tfrac{3}{5}kW_r'^{1/2}(\mathcal{E}' - W_r')^{5/3} \quad \text{for } W_r' > \mathcal{E}' - B_m'. \quad \text{(B4)}$$

3. "Loose" complex.

$$P_r(W_r') = k(\mathcal{E}' - W_r' - \tfrac{2}{5}B_m')B_m'^{2/3} \quad \text{for } W_r' \leq \mathcal{E}' - B_m'$$
$$= \tfrac{3}{5}k(\mathcal{E}' - W_r')^{5/3} \quad \text{for } W_r' > \mathcal{E}' - B_m'. \quad \text{(B5)}$$

Previously Eqs. (B3) and (B4) have been derived by Safron.[37] For Ba + O_2, we have found by comparison of $P_r(W_r')$ calculated using quantum level densities[40] that the use of classical energy level densities does not significantly affect the rotational distributions. This is to be expected since the zero point energies of the reactants, complex, and products are small compared to $\mathcal{E}'$.

Finally we calculate the rotational distribution for one of the two diatomic molecules formed from a 4-atom complex [see Eq. (A2)]. Using classical energy level densities in Eq. (B1), we find with the help of Table III:

1. "Tight" nonlinear complex, form A.

$$P_r(W_r') = kW_r'[(\mathcal{E}' - W_r')^4 - \tfrac{8}{5}(\mathcal{E}' - W_r')^3B_m' + \tfrac{3}{2}(\mathcal{E}' - W_r')^2B_m'^2 - \tfrac{8}{11}(\mathcal{E}' - W_r')B_m'^3 + \tfrac{1}{7}B_m'^4]B_m'^{2/3}$$
$$\text{for } W_r' \leq \mathcal{E}' - B_m'$$
$$= \tfrac{243}{770}kW_r'(\mathcal{E}' - W_r')^{14/3} \quad \text{for } W_r' > \mathcal{E}' - B_m. \quad \text{(B6)}$$

2. "Tight" nonlinear complex, form B.

$$P_r(W_r') = \tfrac{3}{2} k W_r' B_m'^{\,2/3} (\mathcal{E}' - W_r')^{7/2} F(-\tfrac{7}{2}, \tfrac{2}{3}; \tfrac{5}{3}; B_m'/[\mathcal{E}' - W_r']) \quad \text{for } W_r' \le \mathcal{E}' - B_m'$$

$$= k W_r' (\mathcal{E}' - W_r')^{25/6} \Gamma(\tfrac{9}{2}) \Gamma(\tfrac{2}{3}) / \Gamma(\tfrac{31}{6}) \quad \text{for } W_r' > \mathcal{E}' - B_m'. \tag{B7}$$

3. "Loose" complex.

$$P_r(W_r') = k[(\mathcal{E}' - W_r')^3 - \tfrac{6}{5}(\mathcal{E}' - W_r')^2 B_m' + \tfrac{3}{4}(\mathcal{E}' - W_r') B_m'^{\,2} - \tfrac{6}{11} B_m'^{\,3}] B_m'^{\,2/3} \text{ for } W_r' \le \mathcal{E}' - B_m'$$

$$= \tfrac{1}{220} k (\mathcal{E}' - W_r')^{11/3} \text{ for } W_r' > \mathcal{E}' - B_m'. \tag{B8}$$

The formula for a "tight" linear complex has not been given above since it can be simply obtained from Eq. (B6) by dividing by $W_r'^{\,1/2}$. The Gauss hypergeometric function in Eq. (B7) can be evaluated numerically by using an integral representation[41] so that

$$F(-n/2, \tfrac{2}{3}; \tfrac{5}{3}; x) = \frac{2}{3} \int_0^1 t^{-1/3} (1 - xt)^{n/2} \, dt. \tag{B9}$$

Figure 12 has been calculated using the above results. If W^* had been used in place of W_v^* in Eq. (B1), as would be more appropriate, Fig. 12 is expected to be essentially unaffected. While the formulas for transition state theory presented in Eqs. (B3) through (B8) involve more approximations than those of phase space theory (Appendix A), the present rotational distributions have the particular virtue of being simple to compute. Moreover, as found in this study, they have the qualitative features of the experimental distributions.

*Present address: Department of Chemistry, The Johns Hopkins University, Baltimore, MD 21218.
†Present address: Shell Research Limited, Thornton Research Centre, P.O. Box 1, Chester CH1 3SH, England.
‡Present address: Fakultät für Physik, University of Freiburg, D-7800 Freiburg, Germany.

[1]A. Schultz, H. W. Cruse, and R. N. Zare, J. Chem. Phys. 57, 1354 (1972).
[2]C. B. Cosmovici and K. W. Michel, Chem. Phys. Lett. 11, 245 (1971).
[3]J. Fricke, B. Kim, and W. L. Fite, in *Proceedings of the VII ICPEAC, Abstract of Papers* (North-Holland, Amsterdam, 1971), p. 37.
[4]H. J. Loesch and D. R. Herschbach, J. Chem. Phys. (to be published). A brief account is reported in Faraday Disc. Chem. Soc. 55, 385 (1973). See also F. Engelke, thesis, University of Freiburg, Germany, 1974 (unpublished).
[5]S. J. Riley and D. R. Herschbach, J. Chem. Phys. 58, 27 (1973).
[6]S. M. Freund, G. A. Fisk, D. R. Herschbach, and W. Klemperer, J. Chem. Phys. 54, 2510 (1971); H. G. Bennewitz, R. Haerten, and G. Müller, Chem. Phys. Lett. 12, 335 (1971).
[7]C. Maltz, Ph.D. thesis, Harvard University, Cambridge, MA, 1969 (unpublished).
[8]P. J. Dagdigian and L. Wharton, J. Chem. Phys. 57, 1487 (1972).
[9]A. N. Nesmeyanov, *Vapor Pressure of the Elements*, translated by J. I. Carasso (Academic, New York, 1963).
[10]See, for example, P. J. Dagdigian, H. W. Cruse, and R. N. Zare, J. Chem. Phys. 60, 2330 (1974).
[11]H. W. Cruse, P. J. Dagdigian, and R. N. Zare, Faraday Disc. Chem. Soc. 55, 277 (1973).
[12]We thank Prof. W. C. Lineberger for supplying us with a sample of recrystallized dye.
[13]The source of this dye was the IBM Watson Research Center, Yorktown Heights, NY, and the material was made by C. S. Angadiyavar and R. Srinivasan. We are grateful to R. Srinivasan for supplying us with a sample of this dye.
[14]S. E. Johnson, J. Chem. Phys. 56, 149 (1972).
[15]The RKR Franck–Condon factors calculated by T. Wentink, Jr., and R. J. Spindler, Jr., J. Quant. Spectrosc. Radiat. Transfer 12, 129 (1972), have been used here.
[16]See, for example, R. N. Zare, "Rotational Line Strengths: The $O_2^+ b\,{}^4\Sigma_g^- - a\,{}^4\Pi_u$ Band System," in *Molecular Spectroscopy: Modern Research*, edited by K. N. Rao and C. W. Mathews (Academic, New York, 1972).
[17]G. T. Best and H. S. Hoffman, J. Quant. Spectrosc. Radiat. Transfer 13, 69 (1973), have measured relative intensities of some 50 bands of the BaO A–X system using fluorescent scattering of sunlight from a cloud of BaO vapor in the upper atmosphere. Using Franck–Condon factors and r centroids of Ref. 15, they find that the electronic transition moment varies by about 20% for $1.95 < R < 2.10$ Å, where R is the internuclear distance.
[18]A. Lagerqvist, E. Lind, and R. F. Barrow, Proc. Phys. Soc. A 63, 1132 (1950).
[19]R. W. Field, J. Chem. Phys. 60, 2400 (1974).
[20]L. Wharton and W. Klemperer, J. Chem. Phys. 38, 2705 (1963).
[21]R. W. Field, A. D. English, T. Tanaka, D. O. Harris, and D. A. Jennings, J. Chem. Phys. 59, 2191 (1973).
[22]The cross section σ_J for formation of low J states ($J \le 30$) is expected to be proportional to $2J+1$ since the final translational energy and hence S matrix elements are changing slowly with J when J is small. The $2J+1$ term merely is a degeneracy factor. This is derived from phase space theory in Appendix A. There is also experimental evidence for this relation in the infrared chemiluminescence experiments of Polanyi and co-workers [see, for example, K. G. Anlauf, D D. S. Horne, R. G. Macdonald, J. C. Polanyi, and K. B. Woodall, J. Chem. Phys. 57, 1561 (1972)]. We terminate the high J populations in the derived BaO distribution by setting $N_J = 0$ for $J \ge 100$ (see Sec. IIIC on reaction exoergicity).
[23]The least-squares computer programs of P. R. Bevington, *Data Reduction and Error Analysis for the Physical Sciences* (McGraw-Hill, New York, 1969), are used. The scaling factor N relating the absolute intensity of the calculated spectrum to the experimental one is fixed by setting $N = \sum_i I_i y_i / \sum_i y_i^2$, where I_i and y_i are the experimental and calculated intensities at wavelength i, respectively, and the sum is over all wavelengths for which the experimental intensities (peak heights) have been measured. This scale factor N may be shown to be the best one in a least-squares sense.
[24]C. J. Hsu, W. D. Krugh, H. B. Palmer, R. H. Obenauf, and C. F. Aten, J. Mol. Spectry. (to be published).
[25]J. G. Pruett, P. J. Dagdigian, and R. N. Zare (unpublished work presented by H. U. Lee at the First Summer Colloquium on Electronic Transition Lasers, at the University of California at Santa Barbara, June 1974).
[26]B. de B. Darwent, Natl. Bur. Stand. Ref. Data Ser. NSRDS-NBS 31 (1970).
[27]R. N. Zare, Ber. Bunsenges. Physik. Chem. 78, 153 (1974).
[28]J. E. Mayer and M. G. Mayer, *Statistical Mechanics* (Wiley, New York, 1940), p. 444.
[29]C. D. Jonah, R. N. Zare, and Ch. Ottinger, J. Chem. Phys. 56, 263 (1972).
[30]P. Pechukas, J. C. Light, and C. Rankin, J. Chem. Phys. 44, 794 (1966).

[31]J. O. Hirschfelder, C. F. Curtiss, and R. B. Bird, *Molecular Theory of Gases and Liquids* (Wiley, New York, 1954), p. 964.
[32]Reference 31, p. 987.
[33]Reference 31, p. 28.
[34]The ratio of chemi-ionization to total reaction is not known at thermal energies. However, C. E. Young, P. M. Dehmer, S. Wexler, and R. B. Cohen, Bull. Am. Phys. Soc. 19, 70 (1974), have reported for the reaction $Ba + O_2$ observation of Ba^+, BaO^+, and BaO_2^+ chemi-ionization products in the c. m. energy range 0–50 eV, using a velocity-selected sputtered Ba beam and a supersonic O_2 beam. See also R. B. Cohen, C. Young, and S. Wexler, Chem. Phys. Lett. 19, 99 (1973).
[35]S. A. Safron, N. D. Weinstein, D. R. Herschbach, and J. C. Tully, Chem. Phys. Lett. 12, 564 (1972).
[36]R. A. Marcus, J. Chem. Phys. 20, 359 (1952); 43, 2658 (1965); G. M. Wieder and R. A. Marcus, J. Chem. Phys. 37, 1835 (1962); B. S. Rabinovitch and E. V. Waage, Chem. Rev. 70, 377 (1970); O. K. Rice, *Statistical Mechanics, Thermodynamics, and Kinetics* (Freeman, San Francisco, 1967), pp. 495–573; P. J. Robinson and K. A. Holbrook, *Unimolecular Reactions* (Wiley, London, 1972).
[37]S. A. Safron, Ph. D. thesis, Harvard University, Cambridge, Massachusetts, 1969 (unpublished).
[38]R. A. Marcus, Faraday Disc. Chem. Soc. 55, 379 (1973).
[39]R. D. Levine and R. B. Bernstein, J. Chem. Phys. 53, 686 (1970).
[40]The classical energy level density $N_{v\gamma}$ and total state function $W^*_{v\gamma}$ for a group of independent vibrators and free rotators are given by $N_{v\gamma}(E) = kE^{v+\gamma/2-1}$ and $W^*_{v\gamma}(E) = k'E^{v+\gamma/2}$, where v and γ are the number of vibrational and rotational degrees of freedom, respectively, and k and k' are proportionality constants. See W. Forst, Chem. Rev. 71, 339 (1971) for a review of the calculation of both classical and quantum energy level densities and state functions.
[41]I. S. Gradshteyn and I. M. Ryzhik, *Table of Integrals, Series, and Products* (Academic, New York, 1965), p. 1040, Eq. (9.111).